Title
Nanoparticles grown from methanesulfonic acid and methylamine: microscopic structures and formation mechanism.

Journal
Physical chemistry chemical physics : PCCP, 19(47)

ISSN
1463-9076

Authors
Xu, Jing
Finlayson-Pitts, Barbara J
Gerber, R Benny

Publication Date
2017-12-01

DOI
10.1039/c7cp06489f

Peer reviewed

PCCP

PAPER

View Article Online
View Journal

Cite this: DOI: 10.1039/c7cp06489f

Nanoparticles grown from methanesulfonic acid and methylamine: microscopic structures and formation mechanism†

Jing Xu, [a] Barbara J. Finlayson-Pitts [a] and R. Benny Gerber *[ab]

Received 22nd September 2017,
Accepted 20th November 2017

DOI: 10.1039/c7cp06489f

rsc.li/pccp

Mechanisms of particle formation and growth in the atmosphere are of great interest due to their impacts on climate, health and visibility. However, the microscopic structures and related properties of the smallest nanoparticles are not known. In this paper we pursue computationally a microscopic description for the formation and growth of methanesulfonic acid (MSA) and methylamine (MA) particles under dry conditions. Energetic and dynamics simulations were used to assess the stabilities of proposed model structures for these particles. Density functional theory (DFT) and semi-empirical (PM3) calculations suggest that $(MSA–MA)_4$ is a major intermediate in the growth process, with the dissociation energies, enthalpies and free energies indicating considerable stability for this cluster. Dynamics simulations show that this species is stable for at least 100 ps at temperatures up to 500 K, well above atmospheric temperatures. In order to reach experimentally detectable sizes (>1.4 nm), continuing growth is suggested to occur *via* clustering of $(MSA–MA)_4$. The dimer $(MSA–MA)_4\cdots(MSA–MA)_4$ may be one of the smaller experimentally measured particles. Step by step addition of MSA to $(MSA–MA)_4$, is also a likely potential growth mechanism when MSA is excess. In addition, an MSA–MA crystal is predicted to exist. These studies demonstrate that computations of particle structure and dynamics in the nano-size range can be useful for molecular level understanding of processes that grow clusters into detectable particles.

1. Introduction

The formation and growth of particles relevant to the atmosphere has received a great deal of experimental and theoretical attention over the last decade[1] due to their impacts on health,[2–5] visibility[6,7] and climate.[8] Through measurements of the size distributions of the smallest particles, a better understanding of the mechanisms of particle formation and growth has developed.[1,9–23] Thus, gas phase molecules first undergo nucleation to form relatively small stable clusters whose sizes are often below the experimental detection limit, which now approaches 1 nm.[18–20,24] These small clusters subsequently grow into the nanometer range where they can be detected experimentally. However, the microscopic structures and related properties of these nano-size particles are not known.

In order to fully understand the nature of clusters and nanoparticles during nucleation and growth, two classes of theoretical approaches have typically been employed to elucidate at a molecular level properties that are difficult to study experimentally. One method is dynamic modeling which has been applied to the formation of neutral and ionic atmospheric clusters.[25–33] These models describe cluster formation and evaporation rates, concentrations, growth to larger sizes etc., but the microscopic structures of nanoparticles are not established. The second method is quantum chemical calculations which can be used to obtain equilibrium structures, energies and thermochemical parameters, and for which results for a number of small clusters in the atmosphere have been reported.[34–59] These theoretical studies include equilibrium structures,[35–41] transition states,[44,45] formation energies[36,37,46–51] and nucleation rates.[58,59] However, quantum chemical calculations on nano-size clusters have been somewhat limited.[59–63] For example, DePalma *et al.*[60,61] studied nano-size clusters of sulfuric acid (H_2SO_4) and ammonia (NH_3)/dimethylamine (DMA) with and without water. The structures and formation energies of the charged clusters $[(BH^+)_x(HSO_4^-)_y]^{+/-}$ (B = NH_3 or DMA, $x = y + 1$, $1 \le y \le 10$) and the neutral clusters $[(BH^+)_x(HSO_4^-)_x(H_2O)_y]$ (B = NH_3 or DMA, $2 \le x \le 8$, $0 \le y \le 10$) were computed using density functional methods. Similarly, Ortega *et al.*[59,62] reported structures and evaporation rates for negatively and positively charged clusters containing up to four H_2SO_4 and four DMA

[a] Department of Chemistry, University of California, Irvine, CA 92697, USA. E-mail: benny@fh.huji.ac.il; Tel: +1 949 824-6758
[b] Institute of Chemistry, Fritz Haber Research Center, Hebrew University of Jerusalem, Jerusalem 91904, Israel

† Electronic supplementary information (ESI) available. See DOI: 10.1039/c7cp06489f

molecules and up to five H_2SO_4 and five NH_3 molecules. A thermochemical analysis approach to the ternary ionic $(HSO_4^-)(H_2SO_4)_m(NH_3)_k(H_2O)_n$ ($m = n \leq 3$, $k = 1, 2$) clusters was reported by Herb *et al.*[63]

Recently, Finlayson-Pitts and coworkers[64–69] carried out a series of studies on the formation and growth of particles from the reactions of methanesulfonic acid (MSA, CH_3SO_3H) with ammonia and amines, all of which have been measured in the atmosphere.[70–82] Calculations on small clusters of MSA with ammonia or amines have been carried out,[41,42,56,64,65,69] but insight into the structures of the nanoparticles formed is still lacking.

We present here a theoretical, microscopic description for nanoparticles formed in the reaction of MSA with methylamine (MA). The clusters studied are in the smallest size range that could be accessed in the experiments (>1.4 nm).[67] Quantum chemical calculations are carried out to compute structures, energies and related properties of the clusters. The stabilities are further studied by molecular dynamic simulations from low (200 K) to high temperatures (500 K). We discuss potential continuing growth mechanism, and propose models for the structure of particles formed in the experiment. The crystalline structure of MSA–MA particles is also predicted.

The paper is organized as follows. Section 2 describes the methodology. In Section 3, we report quantum chemical and semi-empirical results of nano-clusters that have sizes that could be detected experimentally, and the corresponding crystalline structure. Finally, in Section 4, we summarize our conclusions and discuss directions for future work.

2. Methodology

In acid–base clusters, hydrogen bonds may be formed between the acid and the base, or proton transfer may occur from the acid to the base. A suitable quantum chemical potential for the prediction of the structure of the acid–base cluster should give a good description of hydrogen bonds, van der Waals' interactions and whether the proton transfer reaction takes place. Recent benchmarking studies[83] on the H_2SO_4, NH_3 and DMA system show that Perdew–Burke–Ernzerhof (PBE)[84] density functional performs quite well for prediction of the structures and binding energies. Hence, we employed PBE density functional with the Dunning double-ζ correlation-consistent basis set cc-pVDZ[85] for the structure optimization, vibrational frequencies, energies, enthalpies and Gibbs free energies (at 298 K). To verify the reliability of the PBE/cc-pVDZ results, we took B3LYP-D3/aug-cc-pVDZ and MP2/aug-cc-pVDZ as the references for our test calculations on the smallest system, MSA–MA. The test results showed that proton transfer from MSA to MA was predicted at all three levels of theory, and the geometries of MSA–MA we obtained here were similar to the previous study (see Fig. S1 in ESI†).[57] For the larger systems $(MSA–MA)_4\cdots(MSA–MA)_4$, MSA–$(MSA–MA)_4$ and MA–$(MSA–MA)_4$, all of the calculations were done at the level of PBE/3-21G.[86] Partial charges on each component were calculated to present the charge separation in clusters using natural bond orbital (NBO) analysis.[87,88] In order to compare $(MSA–MA)_4$ with other possible conformations, PACKMOL package[89,90] was employed to generate the conformational sampling. Four MSA molecules and four MA molecules were randomly put into a 10.0 Å × 10.0 Å × 10.0 Å cube. The criterion of distance between each molecule is set to 1.8 Å. Using the program, we generated three hundred different initial structures. These structures were first calculated at the level of PBE/6-31+G(d).[91,92] For those isomers within 10 kcal mol^{-1} of the lowest-energy isomer, we refined the geometries and frequencies at the PBE/cc-pVDZ level. All electronic structure calculations were carried out using the Q-CHEM 4.3 program package.[93]

The processes of nucleation and growth of atmospheric nanoparticles involve competing processes, and these will affect the concentrations of the precursors and the composition of the nanoparticles formed. The energies of clusters obtained through quantum chemical calculations are at 0 K, which may be different from that at room temperature.[94] Although the free energies at 298 K were also computed, the ΔG values only provide the relative thermodynamic stability of the two states being compared. Dynamic stability is of importance, and the dynamic simulations can predict relevant properties, *e.g.*, whether the nano-size cluster will dissociate into other fragments, what the fragments will be, the timescale on which the dissociation takes place, and the temperature dependence of these properties. Hence, in order to verify the dynamic stabilities of the proposed particle models, molecular dynamic simulations were also employed. Because *ab initio* molecular dynamic simulations of the nano-size clusters are expensive, molecular dynamic simulations with semi-empirical quantum chemical potentials (PM3)[95] having lower computational cost were employed. Molecular dynamic simulations at the PM3 level have been successfully used to study atmospheric molecules and related properties including hydration, dissociation, proton transfer reaction, *etc.*,[96–100] but must be with caution since their accuracy is inferior to DFT methods.

In order to evaluate the reliability of PM3 for our clusters, we tested the PM3 method on the MSA–MA system. Test results showed that the geometry obtained at the PM3 level is close to that obtained using density functional methods (see Fig. S1, ESI†). All dynamic simulations at the level of PM3 were carried out using the CP2K package,[101] on the gas-phase *NVT* canonical ensemble with Nose–Hover thermostats.[102,103] We ran five trajectories for each simulation, and each trajectory was propagated for 100 picoseconds (ps) at a time step interval of 1 femtosecond (fs). In considering the possible effect of temperature on stability, four temperatures, *i.e.*, 200 K, 300 K, 400 K and 500 K were chosen. The dynamic simulations for 100 ps at very high temperatures 400 K and 500 K, much above the atmospheric range, were enough to indirectly demonstrate that the clusters can have longer lifetimes at lower temperatures.

In order to explore the possible existence of crystalline MSA–MA, solid periodic boundary conditions calculations on the MSA–MA crystal were done using the Quantum Espresso package.[104] A projector augmented wave (PAW)[105,106] approach and the generalized gradient approximation (GGA)[107] with the Perdew–Burke–Ernzerhof (PBE) functional were employed in

the structure relaxations. This method was tested using the experimentally known MSA–NH_3 crystal structure. The unit cell parameters of MSA–NH_3 we obtained here are very close to the experimental values[108] (see Table S1 in ESI†).

3. Results and discussion

3.1 The 1 : 1 MSA–MA cluster

MSA–MA, the smallest cluster, has been studied theoretically.[57,66] The geometries, bond lengths of hydrogen bonds and partial charges on MSA–MA computed at the level of PBE/cc-pVDZ are shown in Fig. 1. Consistent with previous studies,[57,66] the most stable structure of MSA–MA is an ion pair $[H_3CSO_3]^-[H_3NCH_3]^+$, where MSA transfers one proton to MA. In our previous study, we found proton transfer in the small cluster qualitatively correlates particle formation observed experimentally.[57] Hence, we proposed that proton transfer should exist in the larger MSA–MA clusters.

3.2 Formation of an $(MSA–MA)_4$ cluster

Particle formation and growth are complicated processes, where molecules can form stable clusters and can also be released from these clusters. An ideal model cluster of these processes should be very stable both thermodynamically and dynamically, which can be estimated through energies (at 0 K), free energies (at 298 K) and dynamics simulations at different temperatures. We assume here that growth starts with the 1 : 1 MSA–MA complex, because the MSA–MA ion pairs should be more stable than structures with only hydrogen bonds between the acid and the base. In the first step, two MSA–MA can form $(MSA–MA)_2$, where two ion pairs form a cyclic structure through hydrogen bonds (see Fig. S2, ESI†). However, the size of $(MSA–MA)_2$, (3.32 Å × 9.69 Å × 11.1 Å) is still far from the experimentally detectable range. Hence, we propose a model cluster consisting of four MSA–MA complexes. The optimized structure of $(MSA–MA)_4$ at the PBE/cc-pVDZ level is shown in Fig. 2. The size of $(MSA–MA)_4$ is 9.22 Å × 9.56 Å × 9.36 Å. The structure of $(MSA–MA)_4$ is a closed cage-like structure composed of four ion pairs in which each oxygen atom forms a hydrogen bond with the transferred proton from MSA to MA. The average bond length of the hydrogen bonds is 1.827 Å, and the average partial charge on MA component is δ = 0.79. Hence, this cage-like $(MSA–MA)_4$ can be seen as a nano-size cluster whose stabilities are assessed in the following.

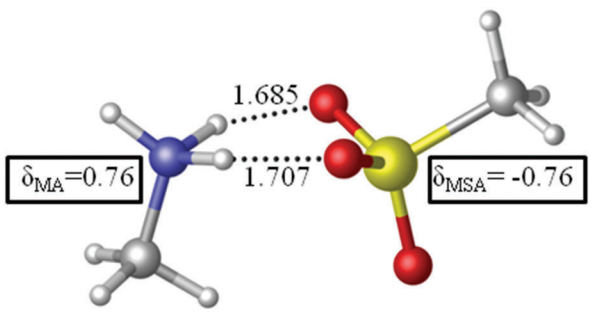

Fig. 1 Key geometrical parameters (Å) and partial charges δ (in atomic units) of MSA–MA at the PBE/cc-pVDZ level. Yellow, red, blue, gray and white spheres represent sulfur, oxygen, nitrogen, carbon and hydrogen atoms, respectively.

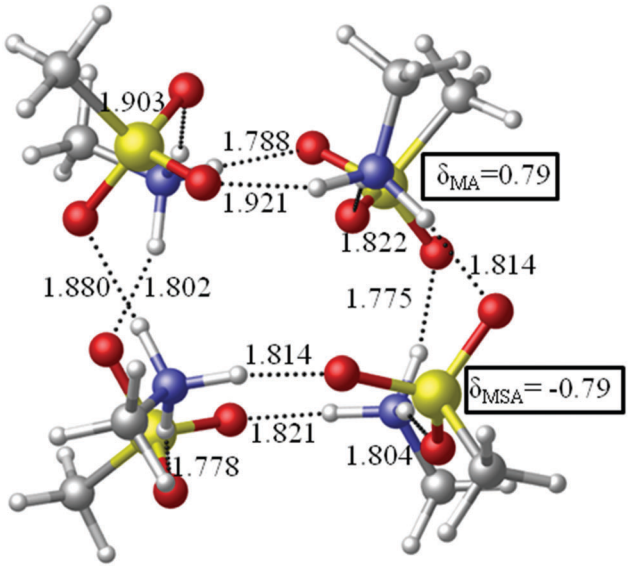

Fig. 2 Key geometrical parameters (Å) and partial charges δ (in atomic units) of $(MSA–MA)_4$ at PBE/cc-pVDZ level.

In order to verify the thermodynamic stability of $(MSA–MA)_4$, we calculated the dissociation energies corrected with zero-point energy, enthalpies and free energies at 298 K (see Table 1). Two possible paths are considered, one that generates four MSA–MA monomers and one that gives two $(MSA–MA)_2$ complexes. When $(MSA–MA)_4$ is directly dissociated to four MSA–MA monomers, the dissociation energy and enthalpy are quite high, *i.e.*, ΔE = 103, ΔH = 101 kcal mol^{-1}. At 298 K, the calculated free energy ΔG is 66.8 kcal mol^{-1}. These positive values show that the dissociation reaction is highly endothermic. Similarly, dissociation of $(MSA–MA)_4$ to two $(MSA–MA)_2$ complexes is also endothermic (ΔE = 34.1, ΔH = 33.8, ΔG = 20.3 kcal mol^{-1}), although less than the dissociation to the MSA–MA monomer. These results demonstrate that $(MSA–MA)_4$ is quite stable thermodynamically. In addition, the dissociation of $(MSA–MA)_2$ to MSA–MA (Table 1) is also endothermic. In short, $(MSA–MA)_4$ is thermodynamically more stable than MSA–MA and $(MSA–MA)_2$.

The dynamic stability of $(MSA–MA)_4$ was verified using dynamic simulations with semi-empirical quantum chemical potentials. At the level of PM3, dynamics simulations of the cage-like structure were carried out at four temperatures: 200 K, 300 K, 400 K, and 500 K. The structures of $(MSA–MA)_4$ at 100 ps are shown in Fig. 3. At each temperature, $(MSA–MA)_4$ does not

Table 1 Dissociation energies with zero-point energy correction (ΔE), enthalpies (ΔH), free energies (in kcal mol^{-1}) at 298 K (ΔG) at PBE/cc-pVDZ level. A positive value means the process is endothermic (ΔE and ΔH) and endergonic (ΔG)

	ΔE	ΔH	ΔG
$(MSA–MA)_4 \rightarrow 4 \times MSA–MA$	103	101	66.8
$(MSA–MA)_4 \rightarrow 2 \times (MSA–MA)_2$	34.1	33.8	20.3
$(MSA–MA)_2 \rightarrow 2 \times MSA–MA$	34.4	33.7	23.2

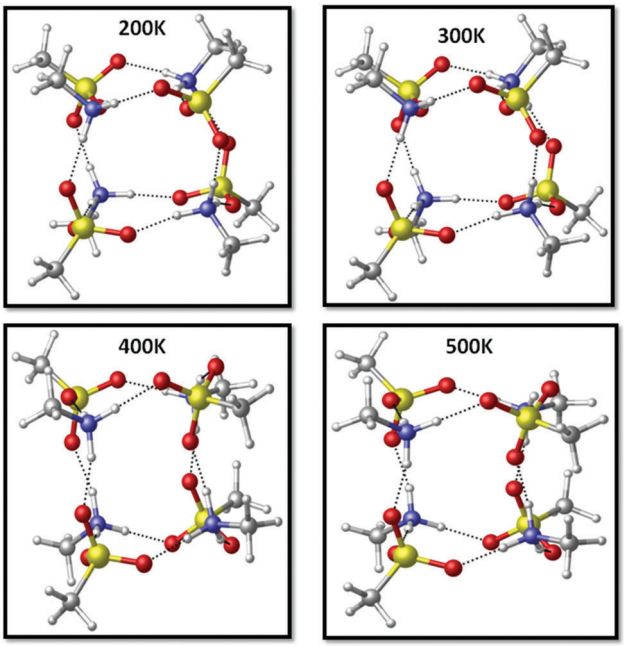

Fig. 3 Structures of $(MSA–MA)_4$ from dynamic simulations at 100 ps at four temperatures (200 K, 300 K, 400 K and 500 K).

change its conformation and still keeps the key cage-like skeleton although the structural parameters change slightly. Each proton transferred from MSA to MA is always bonded with the corresponding MA. Throughout the simulation, the N–H bond lengths (which are ~1.0 Å) do not change significantly with temperature (see Fig. S3, ESI†). The maximum bond lengths are 1.133 (200 K), 1.162 (300 K), 1.191 (400 K) and 1.233 Å (500 K), respectively. In short, from low temperature (200 K) to high temperature (500 K), $(MSA–MA)_4$ always keeps the cage-like structure composed of four ion pairs and is stable for at least 100 ps.

As is typically the case, there are many different local minima in the potential energy surface of the system. Hence, it is useful to verify the stability of $(MSA–MA)_4$ compared with other isomers made of four MSA molecules and four MA molecules. We randomly generated 300 different structures and performed the geometry and frequency calculations. Calculations show that, at the level of PBE/cc-pVDZ, the lowest-energy isomer has the same geometry with our designed $(MSA–MA)_4$. The second isomer is a cyclic structure composed by four ion pairs (see Fig. S4, ESI†), and has 4.71 kcal mol^{-1} higher energy. Dynamic simulations of the second isomer at 300 K shows that the second isomer completely becomes the cage-like $(MSA–MA)_4$ at 8 ps (see Fig. S5, ESI†). Based on these calculations, the results of the random search confirm that $(MSA–MA)_4$ is more stable than other isomers considered here. However, this does not strictly prove that $(MSA–MA)_4$ is the global minimum of the system, it just makes this very likely to be the case.

From the above, the proposed cluster $(MSA–MA)_4$ is very stable both thermodynamically and dynamically. Although the size of $(MSA–MA)_4$ is nearly one nanometer, it is still a little smaller than the experimental detectable size (>1.4 nm). In order to reach the experimental range, possible growth mechanisms of $(MSA–MA)_4$ are proposed.

3.3 Continuing growth of $(MSA–MA)_4$

Now that $(MSA–MA)_4$ has been demonstrated to possess high stability, clustering of $(MSA–MA)_4$ may be a possible method of continuing growth. Here, we take the smallest complex, *i.e.*, the dimer $(MSA–MA)_4\cdots(MSA–MA)_4$ as the example to verify the

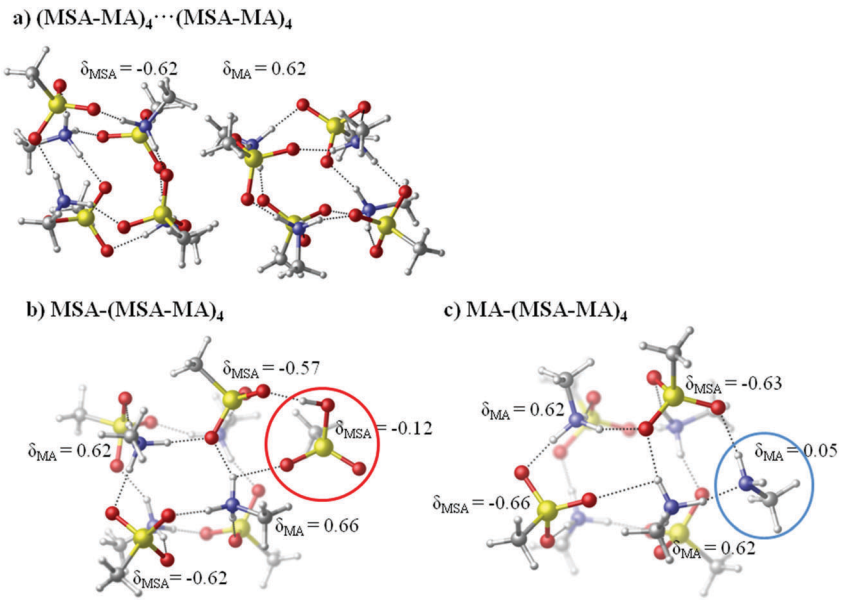

Fig. 4 Structures of (a) $(MSA–MA)_4\cdots(MSA–MA)_4$, (b) $MSA–(MSA–MA)_4$, (c) $MA–(MSA–MA)_4$, and corresponding partial charges δ (in atomic units) at PBE/3-21G level. For $(MSA–MA)_4\cdots(MSA–MA)_4$, the partial charge is the average charge on MSA or MA component. For $MSA–(MSA–MA)_4$ and $MA–(MSA–MA)_4$, inside molecules are blurred out for the better view and only partial charges of outside molecules are shown.

feasibility of this growth mechanism. The structure of the dimer at the PBE/3-21G level is shown in Fig. 4. In $(MSA–MA)_4\cdots(MSA–MA)_4$, two $(MSA–MA)_4$ clusters interact by weak van der Waals forces, and each cluster still has the basic skeleton although the structural parameters change a little. The partial charge on the MA component in the dimer is $\delta = 0.62$, which is about the same as that in $(MSA–MA)_4$ cluster. Note that the average partial charge on the MA component in $(MSA–MA)_4$ at the PBE/3-21G level ($\delta = 0.63$) is smaller than that at PBE/cc-pVDZ level ($\delta = 0.79$).

The corresponding energies of dissociating the dimer to $(MSA–MA)_4$ are listed in Table 2. These positive values, $\Delta E = 22.4$, $\Delta H = 23.1$, $\Delta G = 5.7$ kcal mol^{-1}, indicate the dimer is thermodynamically stable. We also considered the dynamic stability of the dimer using dynamic simulations at the PM3 level carried out for 100 ps at 300 K. The structure of the dimer at 100 ps is shown in Fig. 5. Throughout the simulation, the two cage-like structures sometimes undergo rotation, and the distance between them also changes by a small amount. However, the dynamic simulation results show that the dimer is stable for at least 100 ps at room temperature, although the structure changes slightly.

Table 2 Dissociation energies with zero-point energy correction (ΔE), enthalpies (ΔH), free energies (in kcal mol^{-1}) at 298 K (ΔG) at PBE/3-21G level. A positive value means the process is endothermic (ΔE and ΔH) and endergonic (ΔG)

	ΔE	ΔH	ΔG
$(MSA–MA)_4\cdots(MSA–MA)_4 \rightarrow 2 \times (MSA–MA)_4$	22.4	23.1	5.7
$MSA–(MSA–MA)_4 \rightarrow MSA + (MSA–MA)_4$	23.6	24.2	10.0
$MA–(MSA–MA)_4 \rightarrow MA + (MSA–MA)_4$	15.4	15.4	5.33

In summary, like $(MSA–MA)_4$, the dimer $(MSA–MA)_4\cdots(MSA–MA)_4$ is very stable both thermodynamically and dynamically. The size of the dimer is nearly two nanometers, which is already in the experimental range of detection. Hence, $(MSA–MA)_4\cdots(MSA–MA)_4$ may be one of nanoparticles detected in the experiments, and clustering of $(MSA–MA)_4$ to larger clusters is a feasible mechanism for growth.

Another alternative growth mechanism, *i.e.*, a step by step increase, was also considered. In this kind of growth process, only acid or base molecules monomers are added to $(MSA–MA)_4$, which would represent experiments carried out in excess acid or base. Here, we computed the addition of one MSA or one MA to $(MSA–MA)_4$. The optimized structures of $MSA–(MSA–MA)_4$ and $MA–(MSA–MA)_4$ at PBE/3-21G are shown in Fig. 4. Theoretical calculations show that adding either MSA or MA results in breaking one hydrogen bond in $(MSA–MA)_4$ and formation of a small ring with one ion pair. This extra MSA or MA affects the charge separation, with the contribution of MSA ($\delta = -0.12$) being a little larger than MA ($\delta = 0.05$).

The stabilities of these two complexes were also considered. The results of the thermodynamic calculations for the two complexes are summarized in Table 2. $MSA–(MSA–MA)_4$ and $MA–(MSA–MA)_4$ both have positive dissociation energies (23.6/15.4 kcal mol^{-1}), enthalpies (24.2/15.4 kcal mol^{-1}) and free energies (10.0/5.33 kcal mol^{-1}), indicating good thermodynamic stability. Dynamic simulations show that $MSA–(MSA–MA)_4$ is still stable when simulation is run for 100 ps, but MA dissociated from $MA–(MSA–MA)_4$ in just 3.5 ps (see Fig. 5b and c). It is clear that adding the acid to $(MSA–MA)_4$ is feasible at room temperature, and addition of MSA leads to the growth of particles. However, in order to reach the experimentally detectable size, more MSA is required. Hence, growth of $(MSA–MA)_4$ by

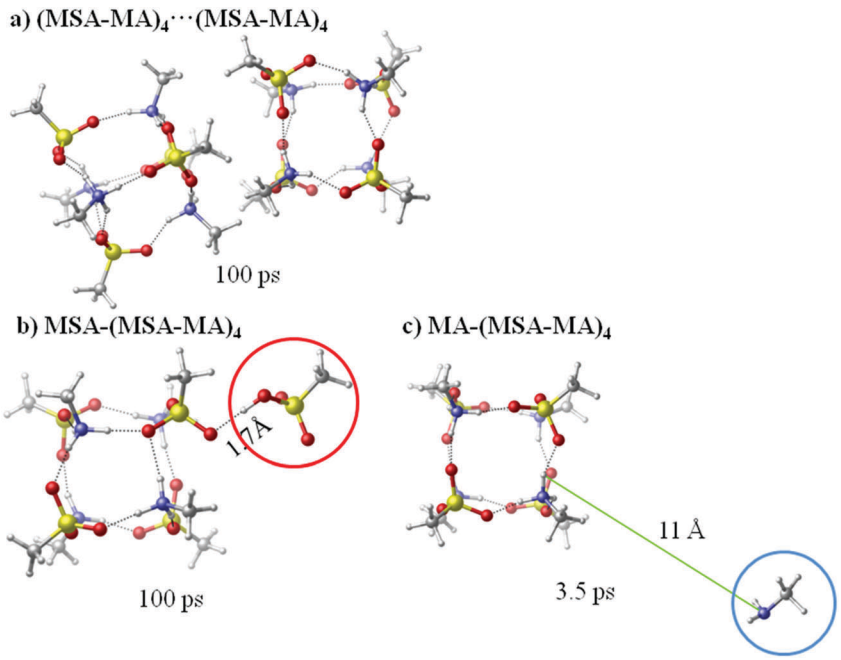

Fig. 5 Snapshots of (a) $(MSA–MA)_4\cdots(MSA–MA)_4$ at 100 ps, (b) $MSA–(MSA–MA)_4$ at 100 ps, and (c) $MA–(MSA–MA)_4$ at 3.5 ps from the dynamic simulations ($T = 300$ K).

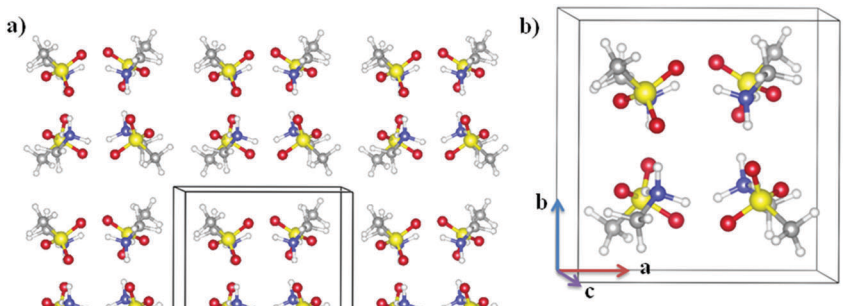

Parameter	Value
a (Å)	9.518
b (Å)	9.531
c (Å)	9.527
α	90.01
β	89.86
γ	90.06

Fig. 6 (a) Crystalline structure of MSA–MA. (b) The unit cell of crystalline MSA–MA. (c) Lattice parameters of the unit cell.

addition of acid molecules is a likely potential growth mechanism when MSA is present in excess in the experiment.

3.4 Does crystalline MSA–MA exist and is it related to $(MSA–MA)_4$?

As discussed above, we found that $(MSA–MA)_4$ involves proton transfer between the MSA and the MA units and has a rigid structure with high symmetry. This raises an interesting conceptual question: can the properties of $(MSA–MA)_4$ also occur for larger MSA–MA particles? Such larger particle could be crystalline MSA–MA. Hence, it is interesting to know whether crystalline MSA–MA exists. Motivated by this, we optimized the cage-like $(MSA–MA)_4$ structure using periodic boundary conditions. The crystal structure and the lattice parameters using PAW-GGA (PBE) approach are shown in Fig. 6. From the values of unit cell parameters, the unit cell of the crystal is very close to a cube. The structure in the unit cell is likewise a cage-like $(MSA–MA)_4$ structure, but obviously has higher symmetry compared with that cluster. For example, in the unit cell, each hydrogen bond has nearly the same bond length, *i.e.*, 1.733 Å, while in $(MSA–MA)_4$, each H-bond is different and the average bond length is 1.827 Å. Thus, our calculations predict the existence of the crystalline MSA–MA, but we cannot claim that it can be formed from $(MSA–MA)_4$ in the atmospheric process of particle growth. As far as we are aware, there is no experimental evidence for this and it may be a very long time-scale process that requires very controlled conditions. However, our predicted MSA–MA crystal can perhaps be prepared in the laboratory, and if this is realized, studies of the crystal may also help for understanding of all MSA–MA clusters and particles.

4. Concluding remarks

In this paper, we designed a cage-like nano-size $(MSA–MA)_4$ cluster. Semi-empirical and *ab initio* quantum chemistry calculations show this cage-like structure possesses very high thermodynamic and dynamic stability, supporting its potential for playing a key role in the process that grows clusters to detectable particles. However, the size of $(MSA–MA)_4$ is somewhat smaller than the experimental size limit of detection of 1.4 nm. In order to reach the detectable size range, growth mechanisms of $(MSA–MA)_4$ were considered. The dimer $(MSA–MA)_4\cdots(MSA–MA)_4$, which approaches the experimentally detectable size range, is very stable both thermodynamically and dynamically and clustering to form larger clusters appears to be a feasible growth mechanism. Thus, $(MSA–MA)_4\cdots(MSA–MA)_4$ may be one of the smaller experimentally measured particles. Step by step addition of MSA to $(MSA–MA)_4$ may also take place in a growth mechanism when MSA is excess. An MSA–MA crystal was also predicted, and it has some structural similarty to $(MSA–MA)_4$, but it is not expected to form in atmospheric conditions. In short, the cage-like $(MSA–MA)_4$ can be seen as a very important intermediate in the formation and growth of MSA–MA particles, and can be used as the building block to form larger particles.

We should note that dry MSA–MA particles are not realistic in the atmosphere because of the ubiquitous presence of water. Previous experimental studies have reported that water enhances MSA–MA particle formation and growth[66,67] which is not treated here. Nevertheless, the microscopic description of the simple binary MSA–MA system may provide preliminary insights into understanding the nature of MSA–MA nanoparticles, and provide a reference for studying the effect of water on nano-size clusters studied in the future.

Conflicts of interest

There are no conflicts to declare.

Acknowledgements

The authors are grateful to the National Science Foundation (grant no. 1443140) and the Israel Science Foundation (grant

no. 172/12) for funding. We thank K. D. Arquero for helpful discussions on the experiments. Computational resources are the Green-planet cluster at University of California, Irvine.

References

1 R. Zhang, A. Khalizov, L. Wang, M. Hu and W. Xu, *Chem. Rev.*, 2012, **112**, 1957–2011.
2 C. A. Pope and D. W. Dockery, *J. Air Waste Manage. Assoc.*, 1995, **2006**(56), 709–742.
3 D. W. Dockery, C. A. Pope, X. Xu, J. D. Spengler, J. H. Ware, M. E. Fay, B. G. J. Ferris and F. E. Speizer, *N. Engl. J. Med.*, 1993, **329**, 1753–1759.
4 J. L. Mauderly and J. C. Chow, *Inhalation Toxicol.*, 2008, **20**, 257–288.
5 J. Lelieveld, J. S. Evans, M. Fnais, D. Giannadaki and A. Pozzer, *Nature*, 2015, **525**, 367–371.
6 W. C. Hinds, *Aerosol Technology: Properties, Behavior, and Measurement of Airborne Particles*, John Wiley & Sons, 2012.
7 A. Singh, W. J. Bloss and F. D. Pope, *Atmos. Chem. Phys.*, 2017, **17**, 2085–2101.
8 T. F. Stocker, D. Qin, G. K. Plattner, M. Tignor, S. K. Allen, J. Boschung, A. Nauels, Y. Xia, B. Bex and B. M. Midgley, *IPCC, 2013: Climate Change 2013: The Physical Science Basis. Contribution of Working Group I to the Fifth Assessment Report of the Intergovernmental Panel on Climate Change*, Cambridge University Press, Cambridge, UK and New York, NY, USA, 2013.
9 B. J. Finlayson-Pitts and J. N. Pitts, Jr., *Chemistry of the Upper and Lower Atmosphere: Theory, Experiments, and Applications*, Academic Press, 1999.
10 M. Kulmala, H. Vehkamäki, T. Petäjä, M. Dal Maso, A. Lauri, V.-M. Kerminen, W. Birmili and P. H. McMurry, *J. Aerosol Sci.*, 2004, **35**, 143–176.
11 J. H. Zollner, W. A. Glasoe, B. Panta, K. K. Carlson, P. H. McMurry and D. R. Hanson, *Atmos. Chem. Phys.*, 2012, **12**, 4399–4411.
12 P. Paasonen, T. Nieminen, E. Asmi, H. E. Manninen, T. Petäjä, C. Plass-Dülmer, H. Flentje, W. Birmili, A. Wiedensohler, U. Hõrrak, A. Metzger, A. Hamed, A. Laaksonen, M. C. Facchini, V.-M. Kerminen and M. Kulmala, *Atmos. Chem. Phys.*, 2010, **10**, 11223–11242.
13 M. Chen, M. Titcombe, J. Jiang, C. Jen, C. Kuang, M. L. Fischer, F. L. Eisele, J. I. Siepmann, D. R. Hanson, J. Zhao and P. H. McMurry, *Proc. Natl. Acad. Sci. U. S. A.*, 2012, **109**, 18713–18718.
14 M. Kulmala, L. Laakso, K. E. J. Lehtinen, I. Riipinen, M. Dal Maso, T. Anttila, V.-M. Kerminen, U. Hõrrak, M. Vana and H. Tammet, *Atmos. Chem. Phys.*, 2004, **4**, 2553–2560.
15 I. Riipinen, S.-L. Sihto, M. Kulmala, F. Arnold, M. Dal Maso, W. Birmili, K. Saarnio, K. Teinilä, V.-M. Kerminen, A. Laaksonen and K. E. J. Lehtinen, *Atmos. Chem. Phys.*, 2007, **7**, 1899–1914.
16 S.-L. Sihto, M. Kulmala, V.-M. Kerminen, M. Dal Maso, T. Petäjä, I. Riipinen, H. Korhonen, F. Arnold, R. Janson, M. Boy, A. Laaksonen and K. E. J. Lehtinen, *Atmos. Chem. Phys.*, 2006, **6**, 4079–4091.
17 J. Boulon, K. Sellegri, Y. Katrib, J. Wang, K. Miet, B. Langmann, P. Laj and J.-F. Doussin, *Aerosol Sci. Technol.*, 2013, **47**, 153–157.
18 M. Kulmala, J. Kontkanen, H. Junninen, K. Lehtipalo, H. E. Manninen, T. Nieminen, T. Petäjä, M. Sipilä, S. Schobesberger, P. Rantala, A. Franchin, T. Jokinen, E. Järvinen, M. Äijälä, J. Kangasluoma, J. Hakala, P. P. Aalto, P. Paasonen, J. Mikkilä, J. Vanhanen, J. Aalto, H. Hakola, U. Makkonen, T. Ruuskanen, R. L. Mauldin, J. Duplissy, H. Vehkamäki, J. Bäck, A. Kortelainen, I. Riipinen, T. Kurtén, M. V. Johnston, J. N. Smith, M. Ehn, T. F. Mentel, K. E. J. Lehtinen, A. Laaksonen, V.-M. Kerminen and D. R. Worsnop, *Science*, 2013, **339**, 943–946.
19 M. Kulmala, I. Riipinen, M. Sipilä, H. E. Manninen, T. Petäjä, H. Junninen, M. D. Maso, G. Mordas, A. Mirme, M. Vana, A. Hirsikko, L. Laakso, R. M. Harrison, I. Hanson, C. Leung, K. E. J. Lehtinen and V.-M. Kerminen, *Science*, 2007, **318**, 89–92.
20 M. Sipilä, T. Berndt, T. Petäjä, D. Brus, J. Vanhanen, F. Stratmann, J. Patokoski, R. L. Mauldin, A.-P. Hyvärinen, H. Lihavainen and M. Kulmala, *Science*, 2010, **327**, 1243–1246.
21 M. Jose Gonzalez-Alvarez, J. Paternoga, K. Breul, H. Cho, M. Z. Roshandel, M. Soleimani and M. A. Winnik, *Polym. Chem.*, 2017, **8**, 2931–2941.
22 H. Chen and E. Ruckenstein, *Soft Matter*, 2012, **8**, 8911–8916.
23 M. Dall'Osto, D. C. S. Beddows, P. Tunved, R. Krejci, J. Ström, H.-C. Hansson, Y. J. Yoon, K.-T. Park, S. Becagli, R. Udisti, T. Onasch, C. D. O'Dowd, R. Simó and R. M. Harrison, *Sci. Rep.*, 2017, **7**, 3318.
24 R. Zhang, G. Wang, S. Guo, M. L. Zamora, Q. Ying, Y. Lin, W. Wang, M. Hu and Y. Wang, *Chem. Rev.*, 2015, **115**, 3803–3855.
25 H. Vehkamäki and I. Riipinen, *Chem. Soc. Rev.*, 2012, **41**, 5160–5173.
26 M. J. McGrath, T. Olenius, I. K. Ortega, V. Loukonen, P. Paasonen, T. Kurtén, M. Kulmala and H. Vehkamäki, *Atmos. Chem. Phys.*, 2012, **12**, 2345–2355.
27 M. Kulmala, *Atmos. Res.*, 2010, **98**, 201–206.
28 T. Yli-Juuti, K. Barsanti, L. Hildebrandt Ruiz, A.-J. Kieloaho, U. Makkonen, T. Petäjä, T. Ruuskanen, M. Kulmala and I. Riipinen, *Atmos. Chem. Phys.*, 2013, **13**, 12507–12524.
29 F. Yu, *Atmos. Chem. Phys.*, 2006, **6**, 5193–5211.
30 F. Yu, *J. Geophys. Res.: Atmos.*, 2006, **111**, D01204.
31 G. K. Schenter, S. M. Kathmann and B. C. Garrett, *Phys. Rev. Lett.*, 1999, **82**, 3484–3487.
32 I. Napari, J. Julin and H. Vehkamäki, *J. Chem. Phys.*, 2009, **131**, 244511.
33 T. Olenius, O. Kupiainen-Määttä, I. K. Ortega, T. Kurtén and H. Vehkamäki, *J. Chem. Phys.*, 2013, **139**, 084312.
34 A. R. Bandy and J. C. Ianni, *J. Phys. Chem. A*, 1998, **102**, 6533–6539.
35 L. J. Larson, A. Largent and F.-M. Tao, *J. Phys. Chem. A*, 1999, **103**, 6786–6792.

36 A. B. Nadykto and F. Yu, *Chem. Phys. Lett.*, 2007, **435**, 14–18.
37 J. C. Ianni and A. R. Bandy, *J. Phys. Chem. A*, 1999, **103**, 2801–2811.
38 H. Henschel, T. Kurtén and H. Vehkamäki, *J. Phys. Chem. A*, 2016, **120**, 1886–1896.
39 H. Henschel, J. C. A. Navarro, T. Yli-Juuti, O. Kupiainen-Määttä, T. Olenius, I. K. Ortega, S. L. Clegg, T. Kurtén, I. Riipinen and H. Vehkamäki, *J. Phys. Chem. A*, 2014, **118**, 2599–2611.
40 K. E. Anderson, J. I. Siepmann, P. H. McMurry and J. VandeVondele, *J. Am. Chem. Soc.*, 2008, **130**, 14144–14147.
41 S. Li, L. Zhang, W. Qin and F.-M. Tao, *Chem. Phys. Lett.*, 2007, **447**, 33–38.
42 I. Napari, M. Kulmala and H. Vehkamäki, *J. Chem. Phys.*, 2002, **117**, 8418–8425.
43 S. Re, Y. Osamura and K. Morokuma, *J. Phys. Chem. A*, 1999, **103**, 3535–3547.
44 J. W. DePalma, B. R. Bzdek, D. P. Ridge and M. V. Johnston, *J. Phys. Chem. A*, 2014, **118**, 11547–11554.
45 J. Liu, S. Fang, Z. Wang, W. Yi, F.-M. Tao and J. Liu, *Environ. Sci. Technol.*, 2015, **49**, 13112–13120.
46 B. Temelso, T. E. Morrell, R. M. Shields, M. A. Allodi, E. K. Wood, K. N. Kirschner, T. C. Castonguay, K. A. Archer and G. C. Shields, *J. Phys. Chem. A*, 2012, **116**, 2209–2224.
47 T. Kurtén, M. R. Sundberg, H. Vehkamäki, M. Noppel, J. Blomqvist and M. Kulmala, *J. Phys. Chem. A*, 2006, **110**, 7178–7188.
48 T. Kurtén, L. Torpo, C.-G. Ding, H. Vehkamäki, M. R. Sundberg, K. Laasonen and M. Kulmala, *J. Geophys. Res.: Atmos.*, 2007, **112**, D04210.
49 V. Loukonen, T. Kurtén, I. K. Ortega, H. Vehkamäki, A. A. H. Pádua, K. Sellegri and M. Kulmala, *Atmos. Chem. Phys.*, 2010, **10**, 4961–4974.
50 A. B. Nadykto, F. Yu, M. V. Jakovleva, J. Herb and Y. Xu, *Entropy*, 2011, **13**, 554–569.
51 I. K. Ortega, N. M. Donahue, T. Kurtén, M. Kulmala, C. Focsa and H. Vehkamäki, *J. Phys. Chem. A*, 2016, **120**, 1452–1458.
52 B. Temelso, T. N. Phan and G. C. Shields, *J. Phys. Chem. A*, 2012, **116**, 9745–9758.
53 L. Wang, *J. Phys. Chem. A*, 2007, **111**, 3642–3651.
54 H. Zhao, X. Jiang and L. Du, *Chemosphere*, 2017, **174**, 689–699.
55 A. B. Nadykto, J. Herb, F. Yu and Y. Xu, *Chem. Phys. Lett.*, 2014, **609**, 42–49.
56 N. Bork, J. Elm, T. Olenius and H. Vehkamäki, *Atmos. Chem. Phys.*, 2014, **14**, 12023–12030.
57 J. Xu, B. J. Finlayson-Pitts and R. B. Gerber, *J. Phys. Chem. A*, 2017, **121**, 2377–2385.
58 I. Napari, M. Noppel, H. Vehkamäki and M. Kulmala, *J. Geophys. Res.: Atmos.*, 2002, **107**, 4381.
59 I. K. Ortega, O. Kupiainen, T. Kurtén, T. Olenius, O. Wilkman, M. J. McGrath, V. Loukonen and H. Vehkamäki, *Atmos. Chem. Phys.*, 2012, **12**, 225–235.
60 J. W. DePalma, D. J. Doren and M. V. Johnston, *J. Phys. Chem. A*, 2014, **118**, 5464–5473.
61 J. W. DePalma, B. R. Bzdek, D. J. Doren and M. V. Johnston, *J. Phys. Chem. A*, 2012, **116**, 1030–1040.
62 I. K. Ortega, T. Olenius, O. Kupiainen-Määttä, V. Loukonen, T. Kurtén and H. Vehkamäki, *Atmos. Chem. Phys.*, 2014, **14**, 7995–8007.
63 J. Herb, Y. Xu, F. Yu and A. B. Nadykto, *J. Phys. Chem. A*, 2013, **117**, 133–152.
64 M. L. Dawson, M. E. Varner, V. Perraud, M. J. Ezell, R. B. Gerber and B. J. Finlayson-Pitts, *Proc. Natl. Acad. Sci. U. S. A.*, 2012, **109**, 18719–18724.
65 H. Chen, M. J. Ezell, K. D. Arquero, M. E. Varner, M. L. Dawson, R. B. Gerber and B. J. Finlayson-Pitts, *Phys. Chem. Chem. Phys.*, 2015, **17**, 13699–13709.
66 H. Chen, M. E. Varner, R. B. Gerber and B. J. Finlayson-Pitts, *J. Phys. Chem. B*, 2016, **120**, 1526–1536.
67 K. D. Arquero, R. B. Gerber and B. J. Finlayson-Pitts, *Environ. Sci. Technol.*, 2017, **51**, 2124–2130.
68 H. Chen and B. J. Finlayson-Pitts, *Environ. Sci. Technol.*, 2017, **51**, 243–252.
69 M. L. Dawson, M. E. Varner, V. Perraud, M. J. Ezell, J. Wilson, A. Zelenyuk, R. B. Gerber and B. J. Finlayson-Pitts, *J. Phys. Chem. C*, 2014, **118**, 29431–29440.
70 H. Berresheim, J. W. Huey, R. P. Thorn, F. L. Eisele, D. J. Tanner and A. Jefferson, *J. Geophys. Res.: Atmos.*, 1998, **103**, 1629–1637.
71 R. J. Hopkins, Y. Desyaterik, A. V. Tivanski, R. A. Zaveri, C. M. Berkowitz, T. Tyliszczak, M. K. Gilles and A. Laskin, *J. Geophys. Res.: Atmos.*, 2008, **113**, D04209.
72 M. Legrand and E. C. Pasteur, *J. Geophys. Res.: Atmos.*, 1998, **103**, 10991–11006.
73 A. Sorooshian, L. T. Padró, A. Nenes, G. Feingold, A. McComiskey, S. P. Hersey, H. Gates, H. H. Jonsson, S. D. Miller, G. L. Stephens, R. C. Flagan and J. H. Seinfeld, *Global Biogeochem. Cycles*, 2009, **23**, GB4007.
74 C. J. Gaston, K. A. Pratt, X. Qin and K. A. Prather, *Environ. Sci. Technol.*, 2010, **44**, 1566–1572.
75 P. K. Quinn, T. L. Miller, T. S. Bates, J. A. Ogren, E. Andrews and G. E. Shaw, *J. Geophys. Res.: Atmos.*, 2002, **107**, AAC 8-1.
76 H. Berresheim, M. Adam, C. Monahan, C. O'Dowd, J. M. C. Plane, B. Bohn and F. Rohrer, *Atmos. Chem. Phys.*, 2014, **14**, 12209–12223.
77 F. L. Eisele and D. J. Tanner, *J. Geophys. Res.: Atmos.*, 1993, **98**, 9001–9010.
78 R. L. Mauldin, C. A. Cantrell, M. Zondlo, E. Kosciuch, F. L. Eisele, G. Chen, D. Davis, R. Weber, J. Crawford, D. Blake, A. Bandy and D. Thornton, *J. Geophys. Res.: Atmos.*, 2003, **108**, 8796.
79 X. Ge, A. S. Wexler and S. L. Clegg, *Atmos. Environ.*, 2011, **45**, 524–546.
80 M. L. Dawson, V. Perraud, A. Gomez, K. D. Arquero, M. J. Ezell and B. J. Finlayson-Pitts, *Atmos. Meas. Tech.*, 2014, **7**, 2733–2744.
81 Y. You, V. P. Kanawade, J. A. de Gouw, A. B. Guenther, S. Madronich, M. R. Sierra-Hernández, M. Lawler, J. N. Smith, S. Takahama, G. Ruggeri, A. Koss, K. Olson, K. Baumann, R. J. Weber, A. Nenes, H. Guo, E. S. Edgerton,

L. Porcelli, W. H. Brune, A. H. Goldstein and S.-H. Lee, *Atmos. Chem. Phys.*, 2014, **14**, 12181–12194.
82 T. C. VandenBoer, A. Petroff, M. Z. Markovic and J. G. Murphy, *Atmos. Chem. Phys.*, 2011, **11**, 4319–4332.
83 H. R. Leverentz, J. I. Siepmann, D. G. Truhlar, V. Loukonen and H. Vehkamäki, *J. Phys. Chem. A*, 2013, **117**, 3819–3825.
84 J. P. Perdew, K. Burke and M. Ernzerhof, *Phys. Rev. Lett.*, 1996, **77**, 3865–3868.
85 T. H. Dunning Jr, *J. Chem. Phys.*, 1989, **90**, 1007–1023.
86 J. S. Binkley, J. A. Pople and W. J. Hehre, *J. Am. Chem. Soc.*, 1980, **102**, 939–947.
87 J. P. Foster and F. Weinhold, *J. Am. Chem. Soc.*, 1980, **102**, 7211–7218.
88 A. E. Reed and F. Weinhold, *J. Chem. Phys.*, 1983, **78**, 4066–4073.
89 L. Martínez, R. Andrade, E. G. Birgin and J. M. Martínez, *J. Comput. Chem.*, 2009, **30**, 2157–2164.
90 J. M. Martínez and L. Martínez, *J. Comput. Chem.*, 2003, **24**, 819–825.
91 G. A. Petersson, A. Bennett, T. G. Tensfeldt, M. A. Al-Laham, W. A. Shirley and J. Mantzaris, *J. Chem. Phys.*, 1988, **89**, 2193–2218.
92 G. A. Petersson and M. A. Al-Laham, *J. Chem. Phys.*, 1991, **94**, 6081–6090.
93 Y. Shao, Z. Gan, E. Epifanovsky, A. T. B. Gilbert, M. Wormit, J. Kussmann, A. W. Lange, A. Behn, J. Deng, X. Feng, D. Ghosh, M. Goldey, P. R. Horn, L. D. Jacobson, I. Kaliman, R. Z. Khaliullin, T. Kuś, A. Landau, J. Liu, E. I. Proynov, Y. M. Rhee, R. M. Richard, M. A. Rohrdanz, R. P. Steele, E. J. Sundstrom, H. L. W. III, P. M. Zimmerman, D. Zuev, B. Albrecht, E. Alguire, B. Austin, G. J. O. Beran, Y. A. Bernard, E. Berquist, K. Brandhorst, K. B. Bravaya, S. T. Brown, D. Casanova, C.-M. Chang, Y. Chen, S. H. Chien, K. D. Closser, D. L. Crittenden, M. Diedenhofen, R. A. D. Jr, H. Do, A. D. Dutoi, R. G. Edgar, S. Fatehi, L. Fusti-Molnar, A. Ghysels, A. Golubeva-Zadorozhnaya, J. Gomes, M. W. D. Hanson-Heine, P. H. P. Harbach, A. W. Hauser, E. G. Hohenstein, Z. C. Holden, T.-C. Jagau, H. Ji, B. Kaduk, K. Khistyaev, J. Kim, J. Kim, R. A. King, P. Klunzinger, D. Kosenkov, T. Kowalczyk, C. M. Krauter, K. U. Lao, A. D. Laurent, K. V. Lawler, S. V. Levchenko, C. Y. Lin, F. Liu, E. Livshits, R. C. Lochan, A. Luenser, P. Manohar, S. F. Manzer, S.-P. Mao, N. Mardirossian, A. V. Marenich, S. A. Maurer, N. J. Mayhall, E. Neuscamman, C. M. Oana, R. Olivares-Amaya, D. P. O'Neill, J. A. Parkhill, T. M. Perrine, R. Peverati, A. Prociuk, D. R. Rehn, E. Rosta, N. J. Russ, S. M. Sharada, S. Sharma, D. W. Small, A. Sodt, T. Stein, D. Stück, Y.-C. Su, A. J. W. Thom, T. Tsuchimochi, V. Vanovschi, L. Vogt, O. Vydrov, T. Wang, M. A. Watson, J. Wenzel, A. White, C. F. Williams, J. Yang, S. Yeganeh, S. R. Yost, Z.-Q. You, I. Y. Zhang, X. Zhang, Y. Zhao, B. R. Brooks, G. K. L. Chan, D. M. Chipman, C. J. Cramer, W. A. G. III, M. S. Gordon, W. J. Hehre, A. Klamt, H. F. S. III, M. W. Schmidt, C. D. Sherrill, D. G. Truhlar, A. Warshel, X. Xu, A. Aspuru-Guzik, R. Baer, A. T. Bell, N. A. Besley, J.-D. Chai, A. Dreuw, B. D. Dunietz, T. R. Furlani, S. R. Gwaltney, C.-P. Hsu, Y. Jung, J. Kong, D. S. Lambrecht, W. Liang, C. Ochsenfeld, V. A. Rassolov, L. V. Slipchenko, J. E. Subotnik, T. V. Voorhis, J. M. Herbert, A. I. Krylov, P. M. W. Gill and M. Head-Gordon, *Mol. Phys.*, 2015, 113, 184–215.
94 G.-L. Hou, X.-B. Wang and M. Valiev, *J. Am. Chem. Soc.*, 2017, **139**, 11321–11324.
95 J. J. P. Stewart, *J. Comput. Chem.*, 1989, **10**, 209–220.
96 Y. Miller, G. M. Chaban, B. J. Finlayson-Pitts and R. B. Gerber, *J. Phys. Chem. A*, 2006, **110**, 5342–5354.
97 Y. Miller and R. B. Gerber, *J. Am. Chem. Soc.*, 2006, **128**, 9594–9595.
98 M. Shmilovits-Ofir and R. B. Gerber, *J. Am. Chem. Soc.*, 2011, **133**, 16510–16517.
99 D. Shemesh and R. B. Gerber, *J. Chem. Phys.*, 2005, **122**, 241104.
100 M. Shmilovits-Ofir, Y. Miller and R. B. Gerber, *Phys. Chem. Chem. Phys.*, 2011, **13**, 8715–8722.
101 J. VandeVondele, M. Krack, F. Mohamed, M. Parrinello, T. Chassaing and J. Hutter, *Comput. Phys. Commun.*, 2005, **167**, 103–128.
102 S. Nosé, *J. Chem. Phys.*, 1984, **81**, 511–519.
103 W. G. Hoover, *Phys. Rev. Gen. Phys.*, 1985, **31**, 1695–1697.
104 P. Giannozzi, S. Baroni, N. Bonini, M. Calandra, R. Car, C. Cavazzoni, D. Ceresoli, G. L. Chiarotti, M. Cococcioni, I. Dabo, A. D. Corso, S. de Gironcoli, S. Fabris, G. Fratesi, R. Gebauer, U. Gerstmann, C. Gougoussis, A. Kokalj, M. Lazzeri, L. Martin-Samos, N. Marzari, F. Mauri, R. Mazzarello, S. Paolini, A. Pasquarello, L. Paulatto, C. Sbraccia, S. Scandolo, G. Sclauzero, A. P. Seitsonen, A. Smogunov, P. Umari and R. M. Wentzcovitch, *J. Phys.: Condens. Matter*, 2009, **21**, 395502.
105 P. E. Blöchl, *Phys. Rev. B: Condens. Matter Mater. Phys.*, 1994, **50**, 17953–17979.
106 G. Kresse and D. Joubert, *Phys. Rev. B: Condens. Matter Mater. Phys.*, 1999, **59**, 1758–1775.
107 J. P. Perdew and Y. Wang, *Phys. Rev. B: Condens. Matter Mater. Phys.*, 1992, **45**, 13244–13249.
108 C. H. Wei, *Acta Crystallogr., Sect. C: Cryst. Struct. Commun.*, 1986, **42**, 1839–1842.